Experimental Verification for Wireless In-Wheel Motor using Synchronous Rectification with Magnetic Resonance Coupling

Motoki Sato [1)4)] **Giuseppe Guidi** [2)] **Takehiro Imura** [3)] **Hiroshi Fujimoto** [1)]

1) The University of Tokyo, 5-1-5 Kashiwanoha, Kashiwa, Chiba, 277-8561 Japan
2) Sintef Energy, PO Box 4761 Sluppen, No-7465 Trondheim Sem Sæland vei 11, Trondheim,Norway
3) The University of Tokyo, 7-3-1, Hongo, Bunkyo-ku, Tokyo 113-8656, Japan
4) Toyo Denki Seizo K.K., 3-8 Fukuura, Kanazawa-ku, Yokohama, Kanagawa, 236-0004 Japan

Presented at the EVTeC and APE Japan on May 26, 2016

ABSTRACT: A new type of in-wheel motor, which receives electric power by wireless power transfer using magnetic resonance coupling and control signals by wireless communication, thus eliminating completely the need for power and signal cables, have been developed. This system is called Wireless In-Wheel Motor (W-IWM). The overall efficiency of W-IWM system has been subject to considerable improvement. In particular, burst fire control was applied to previous generation W-IWM to keep the wheel driving stable. This control made use of asynchronous rectification, resulting in glitches in the controlled variables when the system commutates between motoring and regeneration, due to wireless signal delay. To achieve more efficient control and smooth energy reversal, this paper proposes a novel control method for W-IWM driving by using an application of synchronous rectification. The experimental results of test bench shows the effectiveness of the proposal.

KEY WORDS: EV and HV systems, motor drive system, in-wheel Motor, wireless power transfer

1. Introduction

Electric vehicles (EVs) have received widespread attention in recent years for their lack of environmentally harmful emissions. Moreover, the EV has a very quick torque response provided by motors when compared to conventional vehicle powered by internal combustion engine (1). EVs have several benefits because of their motion controllability. In this respect, the in-wheel motor (IWM) can be considered as the ultimate mobility system (3). Since the IWM can drive each wheel in the vehicle independently, the EV can employ technologies such as anti-slip control of tires and extension of the vehicle mileage through optimal torque distribution (2). However, a major problem of conventional IWMs is that the power cables and signal wires from the vehicle body to the wheel are exposed to harsh environment, and may be damaged due to continuous bending, impact with debris from the road or become brittle because of the freezing in snowy areas (4).

To overcome this problem, the authors have been proposing a system in which the in-wheel motor receives its power wirelessly from the vehicle body. This is called Wireless In-Wheel Motor (W-IWM) (5). This cutting-edge technology eliminates the risk of cable disconnection of IWM and therefore raises the reliability of the whole vehicle system. Since the motor is subject to vibrations depending on the road conditions, misalignment between the motor and the vehicle can occur. Therefore, the preferred method of wireless power transfer is magnetic resonance coupling, which is robust to misalignment between the transmitter and receiver coils (6)(7).

In the case of a constant power load, the secondary side load voltage is unstable (8). Thus, controlling the voltage or the current by electric converters in both transmitter and receiver side is necessary for the good operation of the W-IWM. However, our first implementation of the W-IWM had some issues.

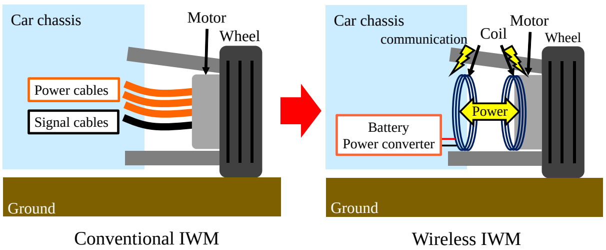

Fig. 1 Concept of W-IWM.

The first problem relates to the behavior of the system in the event of energy reversal that takes place when the motor regenerates. Specifically, glitches are observed on the wheel-side controlled DC-link voltage that are due due to signal communication delay. In fact, in the original implementation, the change in operating mode of the converters on each side of the link was triggered by communication. When regeneration was detected on the wheel-side of the link, a message was sent over the wireless communication channel signaling the converter at the other side to reverse operation from transmitter to receiver of power. Due to considerable communication latency, there was a relatively long interval in which the two sides where both trying to operate as transmitters, resulting in temporary loss of control and consequent accumulation of energy in the DC-link.

Another aspect of the original implementation of the W-IWM system that called for improvement was related to relatively low overall efficiency in the power transfer process between the battery located in the car body and the in-wheel motor. A relatively large share of the losses was due to the use in the in-wheel rectifier of SiC diodes having very high threshold voltage. The new implementation of the W-IWM system presented in this paper makes use of the synchronous rectification concept. By turning on the SiC mosfet devices of the rectifier when the current flow is in the respective anti-parallel diodes, conduction losses can be reduced substantially due to the very low voltage drop across a conducting SiC mosfet compared to the SiC diode [9].

It is shown that, besides the described benefit in terms of efficiency, synchronous rectification can also be used as basis to develop an improved strategy for mode-switching between motoring and regeneration, resulting in smooth and quick power reversal without noticeable glitches on the DC-link voltage. Experimental results related to a test-bench implementation confirm the effectiveness of the proposed technology.

2. the outline of the W-IWM

The concept of in-wheel motor lack of power and signal cables is shown in Fig. 1. Control signal such as torque command send to wheel side wirelessly by Bluetooth. The vehicle for the experiment, FPEV4-*Sawyer*, has been developed in the authors' research team, as shown in Fig. 2(a) [10]. Two inverters are installed in vehicle chassis to handle up to 380 [V] square wave voltage as 85kHz [11]. The resonator composed to coil and capacitor, is connected the output of the inverter for both right and left side at rear sub-flame of car chassis. Consequently, the both inverters which uses SiC MOSFET, drive each resonator and it transmit electric power up to about 3.0kW to receiver resonator in wheel side by magnetic resonant coupling. The gap between transmitter coil and receiver coil is 100 [mm] in this case. The AC/DC converter and PWM inverter which uses SiC MOSFET, is embedded in the motor side. Thus the motor and the converters are electromechanical integrated in the motor in the wheel. The received power as 85 kHz is converted to DC 350 [V] by the AC/DC converter in wheel side. Eventually, the DC-link voltage is inputed to the PWM inverter and the inverter drives the motor. Since this vehicle is the first prototype, the rated power is 6.6kW: motor output is 3.3kW per wheel, and rated wheel torque is 475 Nm. Next target is 12kW per in-wheel and uses four motors at front and rear side. This is equivalent to consumer light car. The author's research team has been already achieved to test run as actual driving.

The concept of in-wheel motor, showing the complete absence of power and signal cables is shown in Fig. 1. Control signals such as torque command are send to wheel side wirelessly by Bluetooth.

The vehicle for the experiment, FPEV4-*Sawyer*, has been developed by the authors' research team and is shown in Fig. 2(a). Two inverters are installed in the vehicle chassis, each able to output up to 380 [V] square wave voltage at 85kHz. The resonators are composed of coils and capacitors and are connected to the output of the inverters for both right and left side at the rear sub-frame of car chassis. Both inverters use SiC mosfets and are each able to transmit up to about 3.0kW of electric power to the respective receiver resonator placed on the wheel side by using the principle of magnetic resonant coupling. The gap between transmitter coil and receiver coil is 100 [mm] in this case. The AC/DC converter and PWM inverter which uses SiC MOSFET is embedded in the motor side. Thus, the motor and the converters are electromechanically integrated with the wheel. The received power at 85 kHz is converted to DC at 350 V by the AC/DC converter in wheel side. Eventually, the DC-link voltage is input to the PWM inverter that drives the motor. Since this vehicle is the first prototype, the rated power is limited to 6.6kW, meaning that

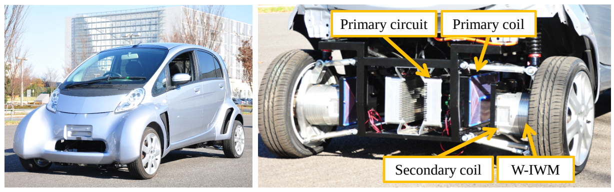

(a) FPEV4-*Sawyer* (b) First trial unit

Fig. 2 Test vehicle and prototype unit.

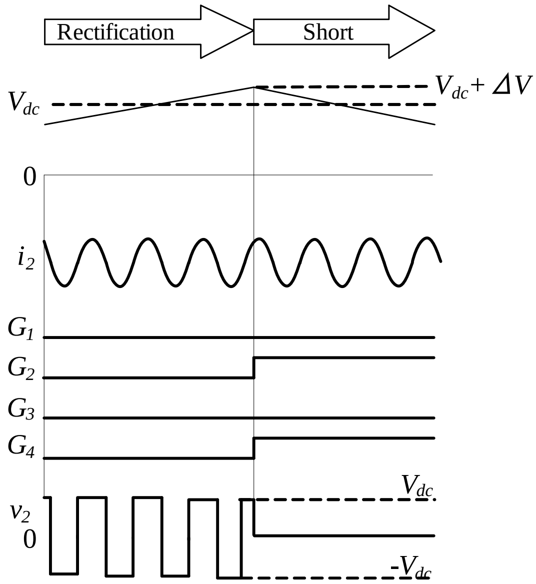

Fig. 4 conventional concept.

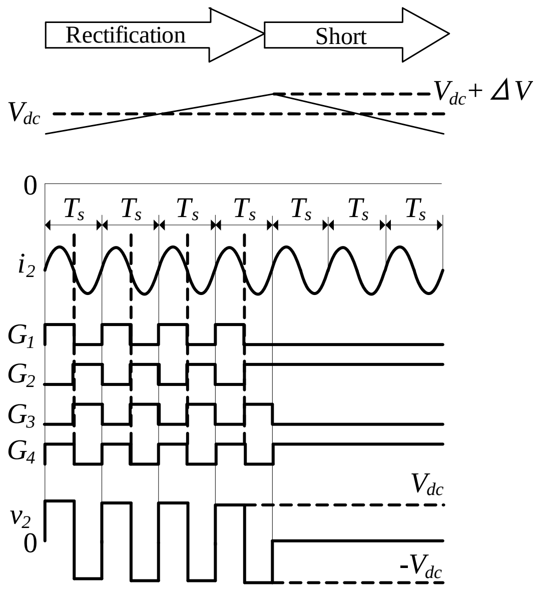

Fig. 5 proposal concept.

motor output is 3.3kW per wheel, and rated wheel torque is 475 Nm. The author's research team has already succeeded in actual test driving of the first vehicle prototype.

Next target is to increase the power rating to 12kW per-wheel and use four motors, meaning one for each wheel. This will give an installed power equivalent to what is normally required by a consumer light car.

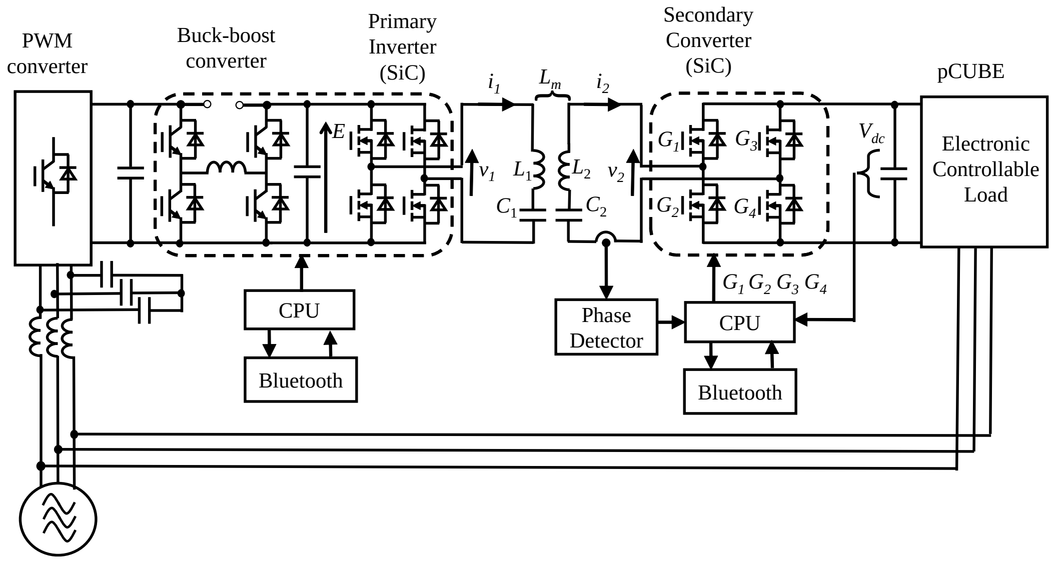

Fig. 3 Schematic of test bench.

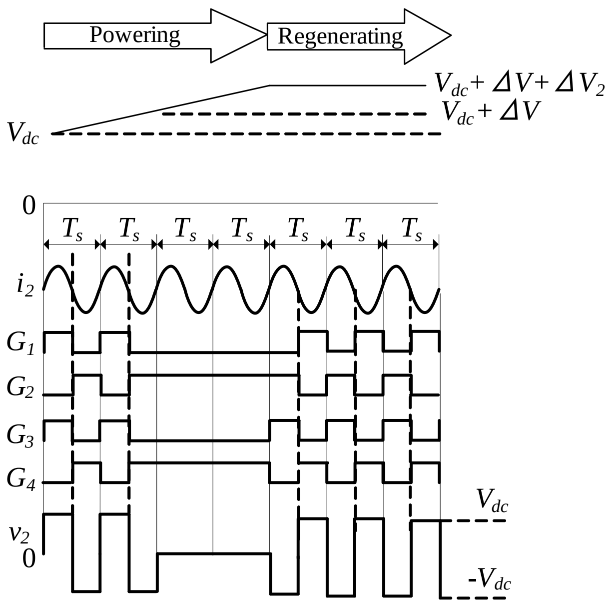

Fig. 6 proposal concept (Regeneration mode).

3. The concept of proposed control

This section shows the schematic diagram of the test bench in Fig. 3. As mentioned above, to achieve stable motor control, on-off control (burst fire control) by using hysteresis comparator is applied in secondary converter. Fig. 4 shows the concept of hysteresis control of secondary converter. The operation is based on the fact that in the configuration in use the secondary coil behaves as current source [12]. When the DC-link voltage reaches the upper limit, the secondary converter makes a short circuit by activating gate signals G_2 and G_4. As a consequence, the current flowing in the receiver coil does not reach the DC-link capacitor, resulting in zero power transfer and causing the voltage of the DC-link to be discharged by the load. After some time the voltage reaches the lower limit. Then, all gate signals G_1, G_2, G_3, G_4 are deactivated and the secondary converter behaves as a diode bridge. The circuit rectifies the 85 kHz AC signals, transferring power to the DC-link and causing the voltage to rise. The DC-link voltage is therefore maintained between the upper and lower limit by alternating the short/rectifier states described before.

This conventional scheme has several merits and some drawbacks. The merits can be listed as follows

- Robust to misalignment
- Simple scheme
- Almost zero switching losses in the rectifier

On the other hand, the demerits are listed as follows

- High conduction loss in the rectifier
- Needs hand shake when switching from powering to regeneration.
  (Energy reversal cannot be achieved smoothly.)

In order to solve these problems, this paper proposes the intermittent synchronous rectification control. Fig. 5 shows the conceptual operation of the proposed method. The main differences with the previous method are that the mosfets are operated during rectifier mode in order to achieve synchronous rectification, thus reducing conduction losses, and that transition between short mode and rectification mode are synchronized with the zero-crossing of the current, thus improving transients. In the figure, T_s is the sampling time, corresponding to 85kHz. The proposed method has merits as follows.

- During rectification, since voltage drop across the SiC mosfet is lower than the one of the anti-parallel diode, losses are reduced and efficiency is improved.
- The proposed method is able to perform energy reversal operation smoothly.

Fig. 6 shows the sequence when the power flow reverses, going from motoring to regeneration. When the DC-link voltage rises, in spite of the rectifier being in short-mode, and reaches the new voltage limit that is higher than the normal threshold level $V_{dc} + \Delta V$, the controller is able to reverse the power flow by inverting the polarity of the switching compared to powering. As a result, the proposed method is able to reverse the energy flow smoothly, without having to wait for information from the chassis-side converter.

However, in order to implement this strategy, the controller needs the additional information of the phase of the coil current

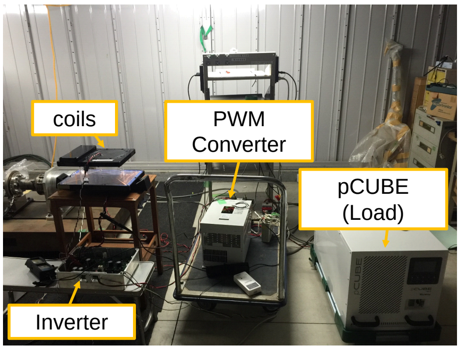

Fig. 7 Experimental setup.

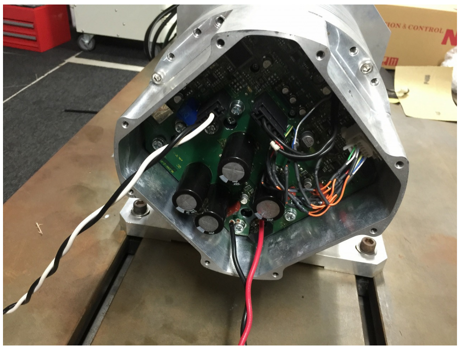
Fig. 8 Secondary motor and circuits.

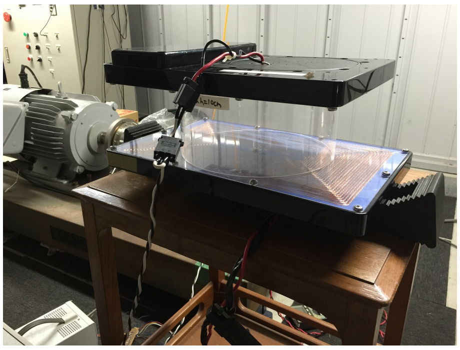
Fig. 9 Resonator.

i_2, which was not needed in the original implementation.

4. Experimental results

4.1. Experimental setup

Fig. 7 shows the experimental setup. In this case, a bidirectional, PWM-based active rectifier supplied by three phase 200 [Vrms] utility grid is used to emulate the on-board battery.

Fig. 8 shows the in-wheel motor assembly, including the embedded converter-inverter circuit.

The motor shown is the actual in-wheel motor used in the test vehicle. However, in this paper, the motor is not operated and wheel-side rectifier is loaded by using pCUBE (product by Myway Plus Corporation, Japan). The latter is a bidirectional, electronically controlled load/supply that is able to emulate constant power as well as constant resistance loads.

Fig. 9 shows the resonator, composed by coils and capacitors. The gap between coils is set to 100 [mm] as in the actual W-IWM system.

4.2. Experimental Results

Fig. 10 shows the voltage and current transients that take place when the state of the in-wheel rectifier is switched from short-circuit to diode-bridge, as a result of hysteresis-based DC-link voltage control, in case of the previous method where the state transitions took place immediately when the DC-link voltage reached the corresponding threshold.

As a comparison, Fig. 11 shows the same voltage and current transients when the proposed control based on synchronization with the rectifier current is used. The proposed method results in slightly faster settling time for the current at the wheel side after a state transition of the rectifier. It can be verified that the current at wheel side is the same during the two modes, while the current at the chassis side changes between almost zero during rectifier short state (no power transferred to the wheel) to the rated value when the rectifier on the wheel side is active.

The two methods give rise to very similar waveforms in steady state, as shown in Fig. 10(b), Fig. 11(b) for the chassis-side and Fig. 10(d), Fig. 11(d) for the wheel-side. This had to be expected, since in steady state the two methods are theoretically equivalent if synchronous rectification is performed correctly.

Fig. 12 shows the magnified figures around the transition instant when the rectifier switches its state from short-circuit to rectifier (Fig. 12(a), Fig. 12(c)) and vice-versa (Fig. 12(b), Fig. 12(d)). It can be noticed that in case of the original control method, since the state transitions are not synchronized with the zero-crossing of the rectifier current, occasional switching of the devices at rather high current may take place. Moreover, some erratic commutation of the passive diode bridge is observed when exiting the short-circuit state, resulting from the rather severe transient on the current that causes spurious zero-crossings. The new control method solves those problems. As a result of synchronization between zero-crossing of the current and switching of the rectifier, zero-current switching (or at least switching with very low current) is achieved even during state transitions.

Fig. 13 shows the smooth transitions between motoring and regeneration modes achieved by the proposed method. The figure shows that when power flow is reversed, going from motoring to regeneration (Fig. 13(b)) and vive-versa (Fig. 13(a)), the DC-link voltage is successfully kept to its set-point of 350[V], without noticeable disturbance.

In contrast, the previous method, based on communication only, was not be able to reverse the power when the rate of change of the latter was as quick as the one in the figure, and only slow transitions between motoring and regenerating were allowed. If the same rate of power change was attempted using the previous method, the system would trip for over voltage in the DC-link caused by the excess power sent by the active load (pCUBE), as the in-wheel converter could not switch quickly enough from rectifier mode to inverter mode. For this reason, the authors could not obtain meaningful experimental results showing energy reversal with the previous method that could be compared with those obtained with the proposed one.

5. Conclusion

This paper proposes a novel control scheme for the wireless in-wheel motor application, based on synchronized switching of the wheel-side rectifier between short-circuit state and rectifier state. This method improves on the hysteresis-based control that was previously employed. In particular, smooth and quick transition between powering and regenerating modes are made possi-

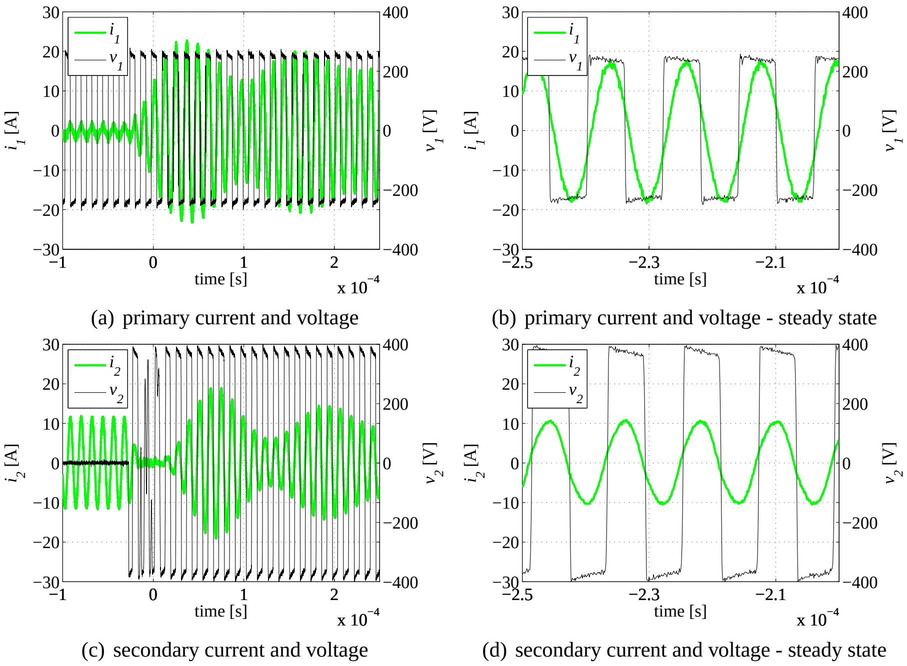

(a) primary current and voltage
(b) primary current and voltage - steady state
(c) secondary current and voltage
(d) secondary current and voltage - steady state

Fig. 10 Experimental results of original hysteresis Control.

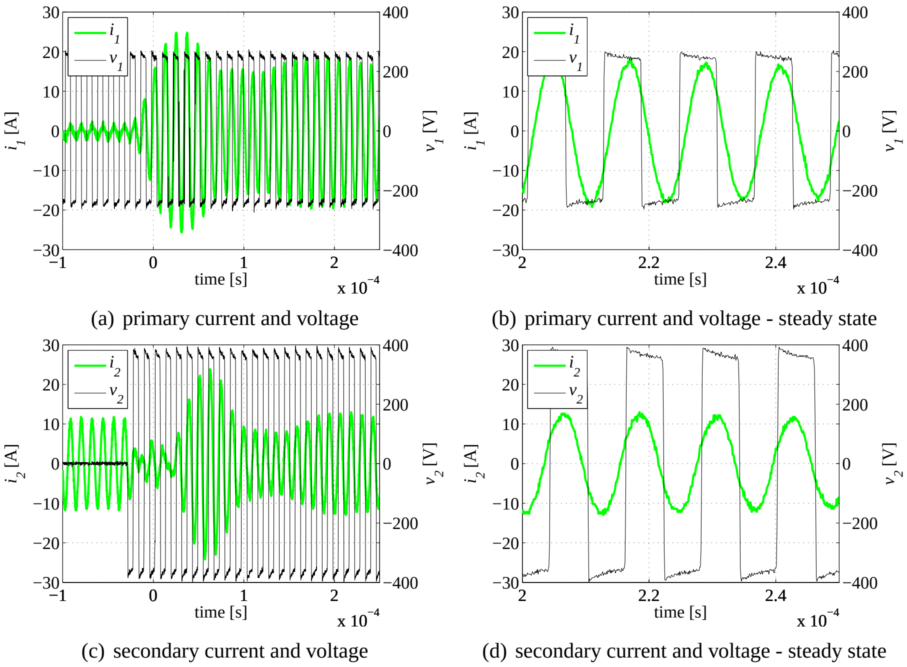

(a) primary current and voltage
(b) primary current and voltage - steady state
(c) secondary current and voltage
(d) secondary current and voltage - steady state

Fig. 11 Experimental results of Proposed Control.

ble. The method also improves the voltage and current transients that appear when the wheel-side rectifier switches between the operating states. Due to the use of synchronous rectification at wheel-side, which is enabled by the tracking of the zero-crossing of the current, the method also achieves higher efficiency than the previous implementation. The efficiency of proposed control is over 94% at rated power (3.3kW). The experimental results taken on a test bench prove the effectiveness of the proposed technology.

Acknowledgment

The research presented in this paper was funded in part by the Ministry of Education, Culture, Sports, Science and Technology grant (No. 26249061). The authors would like to express their deepest appreciation to the Murata Manufacturing Co., Ltd. for providing the laminated ceramic capacitors (U2J characteristics) used in these experiments.

References

(1) Y. Hori: "Future Vehicle Driven by Electricity and Control Research on Four Wheel Motored" UOT Electric March II"", IEEE Trans. IE, Vol. 51, No. 5, pp. 954–962 (2004)

(2) S. Harada, H. Fujimoto: "Range Extension Control System for Electric Vehicles During Acceleration and Deceleration

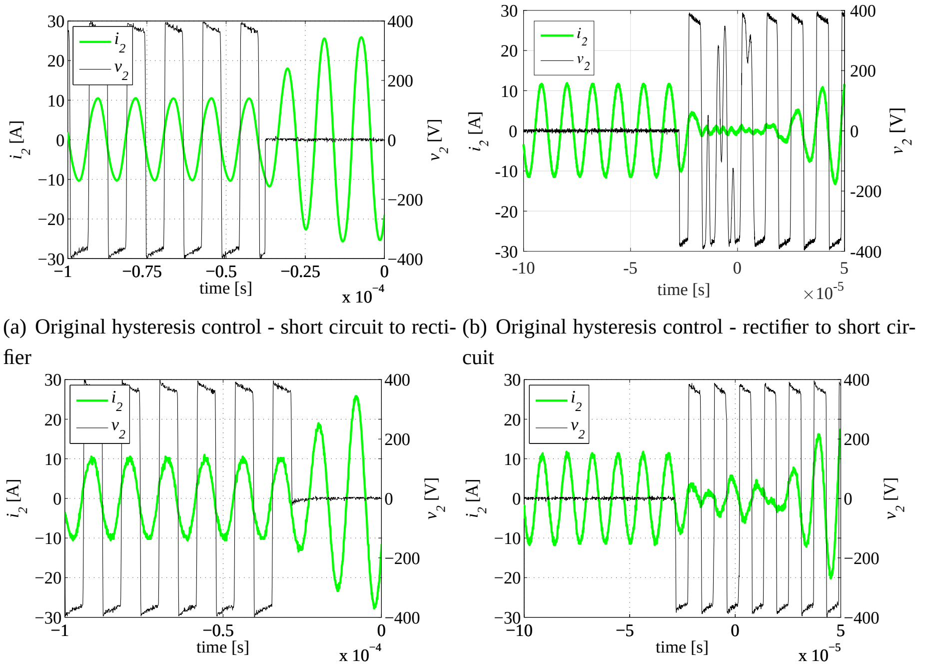

(a) Original hysteresis control - short circuit to rectifier (b) Original hysteresis control - rectifier to short circuit

(c) Proposed control - short circuit to rectifier (d) Proposed control - rectifier to short circuit

Fig. 12 Experimental results of Original control and Proposed control - Comparison of transients

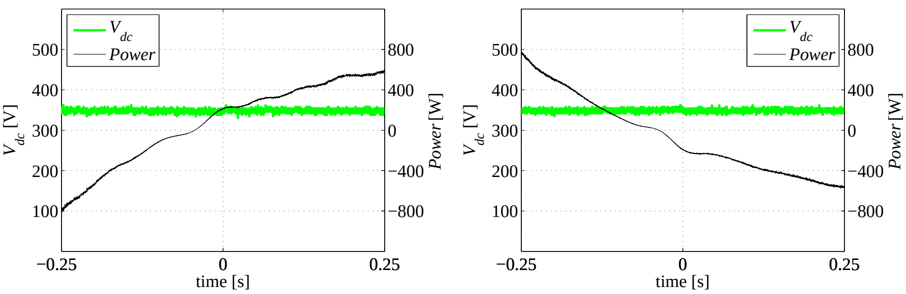

(a) From regeneration to powering. (b) From powering to regeneration

Fig. 13 Experimental results of power flow inversion.

based on Front and Rear Driving-braking Force Distribution Considering Slip Ratio and Motor Loss" In Industrial Electronics Society , (IECON) 2013-39th Annual Conference of the IEEE, pp. 6626-6631.

(3) S. Murata: "Vehicle Dynamics Innovation with In-Wheel Motor," Proc. JSAE EVTeC'11, 20117204, Yokohama, (2011).

(4) Toyota Motor Corporation, P2012–223041A 2012. (in Japanese)

(5) Motoki Sato, Gaku Yamamoto, Takehiro Imura, Hiroshi Fujimoto: "Experimental Verification of Wireless In-Wheel Motor using Magentic Resonance Coupling'', The 9th International Conference on Power Electronics - ECCE Asis, Seoul, Korea, pp.1-6, (2015)

(6) A. Kurs, A. Karalis, R. Moffatt, J. D. Joannopoulos, P. Fishe, and M. Soljacic: "Wireless Power Transfer via Strongly Coupled Magnetic Resonances", in Science Express on 7 June 2007, Vol. 317, No. 5834, pp. 83–86 (2007)

(7) T. Imura, H. Okabe, T. Uchida, and Y. Hori: "Flexibility of Contactless Power Transfer using Magnetic Resonance Coupling to Air Gap and Misalignment for EV", IEEE Electric Vehicle driven on Electric Vehicle Symposium 24, (2009).

(8) D. Gunji, T. Imura, H. Fujimoto, "Fundamental Research on Control Method for Power Conversion Circuit of Wireless In-Wheel Motor using Magnetic Resonance Coupling", IEEJ Transaction on Industry Applications, Vol. 135 No. 3 P 182-191 (2015)

(9) ROHM Co., Ltd. : "bsm120d12p2c005 datasheet", `http://rohmfs.rohm.com/en/products/databook/datasheet/discrete/sic/power_module/bsm120d12p2c005.pdf`

(10) H. Fujimoto, T. Miyajima, and J. Amada: "Development of Electric Vehicle with Variable Drive Unit System", International Electric Vehicle Technology Conference & Automotive Power Electronics Japan 2014 (2014)

(11) SAE International: "Wireless charging advances with selection of 85-kHz charging frequency", `http://articles.sae.org/12647/` (2013)

(12) M. Kato, T. Imura, and Y. Hori: "The Characteritics when Changing Transmission Distance and Load Value in Wireless Power Transfer via Magnetic Resonance Coupling", IEEE Telecommunications Energy Conference INTELEC (2012)